

**The LUCIAE model predictions  
on the light vector meson production in  
proton-proton, proton-nucleus and nucleus-nucleus  
collisions at 158 A GeV**

M. Atayan, H. Gulkanyan

Yerevan Physics Institute, Armenia

**Abstract**

The LUCIAE model predictions are compared with experimental data on light vector meson ( $\rho, \omega, \phi$ ) production in pp, p+Pb and Pb+Pb collisions at 158 A GeV. The model reproduces the general trends of the data, but fails in describing the yield of high- $p_T$  vector mesons in the central Pb+Pb collisions. Predictions for In+In and p+A (A varying from Be to U) collisions at 158 A GeV are also presented.

# 1 Introduction

The enhancement of the strange quark production in heavy ion collisions, in particular, the enhanced yield of  $\phi$  meson relative to non-strange  $\rho$  and  $\omega$  mesons is suggested as a possible signature of quark-gluon plasma (QGP) formation [1, 2]. On the other hand, such an enhancement is also predicted by conventional (no QGP) models, in particular, by the LUCIAE [3], an updated version of the FRITIOF model [4, 5].

The first and most detailed experimental data on the light vector meson ( $\rho, \omega, \phi$ ) production in nuclear collisions are obtained at the CERN SPS. However, up to now no attempt was undertaken to describe simultaneously these data in the framework of a unique approach.

In this Note, the LUCIAE model is employed (with somewhat updated parameters) to compare the theoretical predictions with the existing data on  $\phi$  and  $(\rho + \omega)$  production in pp, p+Pb and Pb+Pb collisions at 158 A GeV [6, 7]. In Section 2, the parameters governing the strange particle yield and the transverse momentum distribution of produced hadrons are described. Section 3 is devoted to the comparison of the model predictions with experimental data. Predictions for In+In and p+A (A varying from Be to U) collisions are also presented. The results are summarized in Section 4.

## 2 The model parameters

The choice of the LUCIAE model parameters governing the multiplicity and transverse momentum distributions of final particles produced in nucleon-nucleon (hadron-nucleon) collisions at SPS energies is motivated in [8] from the comparison with experimental data. The following values of parameters, some of which differ from the default ones [5], will be used below:

- The minimum transverse momentum  $q_{Tmin}$  transferred during the (semi)hard scattering of partons of the colliding hadrons is  $q_{min} \equiv \text{VFR}(12) = 0.6 \text{ GeV}/c$ ;
- The width of the Gaussian distribution of the soft transverse momentum transfer  $Q_T$  between the two colliding hadrons (strings) is given by  $\langle Q_T^2 \rangle \equiv \text{VFR}(6) = 0.1 (\text{GeV}/c)^2$ ;
- The width of the Gaussian distribution of the primordial transverse momentum  $Q_{2T}$  carried by the string ends (valence quark or diquark) is given by  $\langle Q_{2T}^2 \rangle \equiv \text{VFR}(7) = 0.1 (\text{GeV}/c)^2$ ;
- The width of the Gaussian distribution of the transverse momentum ( $p_x$  and  $p_y$  in the string reference frame) acquired by hadrons as a results of the string fragmentation is  $\sigma_x = \sigma_y \equiv \text{PARJ}(21) = 0.405 \text{ GeV}/c$ , equal to the default value [5].

In the LUCIAE model, the broadening of the transverse momentum  $p_T$  distribution in nuclear collisions is suggested to be caused by a novel ('firecracker') mechanism for gluon emission by a high-density collective state formed by several overlapping strings [9]. Besides, a phenomenological mechanism is introduced for the enhancement of the strange quark yield in the fragmentation of the collective string states [10].

The model basic parameters governing the yield of hadrons with strange content are:  $\text{PARJ}(2) = P(s)/P(u)$ , the rate of the  $(s\bar{s})$  production compared to  $(u\bar{u})$  or  $(d\bar{d})$  production, and  $\text{PARJ}(3) = (P(us)/P(ud))/(P(s)/P(d))$ , the extra suppression of the strange diquark production compared to the normal suppression of strange quarks.

For 200 GeV pp collisions, these parameters are tuned in [10] by comparison with data on the strange particle production:  $\text{PARJ}(2) = 0.2$ ,  $\text{PARJ}(3) = 0.3$ . At these values, however, the

model prediction [11] for the  $\phi$  meson average multiplicity  $\langle n_\phi \rangle$  in 158 GeV pp collisions somewhat (by 18%) overestimates the experimental value [6]. Below (in Section 3) we will, therefore, use for 158 GeV pp collisions a slightly smaller value for PARJ(2) = 0.19, keeping the value of PARJ(3) = 0.3.

Below two options of the model are considered: without and with the final state interactions(FSI).The latter includes the following inelastic reactions involving  $\rho$  and/or  $\omega$  mesons:  $\pi N \rightleftharpoons \rho N$ ,  $\bar{N}N \rightarrow \rho\omega$  and  $\bar{Y}N \rightarrow K^*\omega$  ( $Y = \Lambda$  or  $\Sigma$ ), leading to an increased yield of  $\omega$ , especially in heavy ion collisions (however, practically not influencing the yield of  $\rho$ ), while the FSI effects on the  $\Phi$  meson production are neglected [3, 11]. To trace the predicted FSI effects concerning the yield of  $\rho$  and  $\omega$ , the predictions are presented below for both model options.

Note finally, that in the model predictions the following branching ratios for  $\phi$ ,  $\rho$  and  $\omega$  dimuon decay are used:  $B_\phi^{\mu\mu} = (2.87 \pm 0.22) \cdot 10^{-4}$ ,  $B_\rho^{\mu\mu} = (4.60 \pm 0.28) \cdot 10^{-5}$  [12] and  $B_\omega^{\mu\mu} \approx B_\omega^{ee} = (7.07 \pm 0.19) \cdot 10^{-5}$  [13]. The quoted errors of the branching ratios are taken into account in calculations.

### 3 The model predictions and comparison with experimental data

In Table 1 the model predictions for the total average multiplicity  $\langle n_\phi \rangle$  and the  $\langle n_\phi \rangle / \langle n_\pi \rangle$  ratio are compared with the NA49 data [6]. An agreement is seen both for pp, p+Pb and central (at  $b < 3.5$  fm) Pb+Pb data. The predictions for 158 A GeV In+In collisions are also presented.

Reaction	$\langle n_\phi \rangle$	$\langle n_\phi \rangle / \langle n_\pi \rangle$
pp		
NA49	$(1.20 \pm 0.15) \cdot 10^{-2}$	$(0.42 \pm 0.05) \cdot 10^{-2}$
LUCIAE	$(1.39 \pm 0.04) \cdot 10^{-2}$	$(0.46 \pm 0.02) \cdot 10^{-2}$
p+Pb		
NA49	–	$(0.70 \pm 0.09) \cdot 10^{-2}$
LUCIAE	$(4.7 \pm 0.2) \cdot 10^{-2}$	$(0.75 \pm 0.03) \cdot 10^{-2}$
In+In		
LUCIAE	$0.85 \pm 0.01$	$(0.94 \pm 0.01) \cdot 10^{-2}$
Pb+Pb (central)		
NA49	$7.6 \pm 1.1$	$(1.24 \pm 0.18) \cdot 10^{-2}$
LUCIAE	$7.00 \pm 0.04$	$(1.13 \pm 0.01) \cdot 10^{-2}$

Table 1: The multiplicity  $\langle n_\phi \rangle$  and the ratio  $\langle n_\phi \rangle / \langle n_\pi \rangle = 2 \langle n_\phi \rangle / \langle n_{\pi^+ + \pi^-} \rangle$

The model approximately reproduces the pp data [6] on the  $\phi$  meson rapidity (Fig. 1) and transverse mass  $M_T$  (Fig. 2) distributions. The agreement with data for the both distributions is somewhat better than in the original paper [11], where the predictions for the  $\phi$ -production are presented for the first time in the framework of the LUCIAE model, with somewhat different set of parameters mentioned above in Section 2.

The comparison with data for Pb+Pb central collisions [6] is also shown in Figs. 1 and 2. The model overestimates by  $\sim 20\%$  the data at mid-rapidity and predicts somewhat narrower  $y$ -distribution (with width  $\sigma_y = 0.97 \pm 0.02$ ), than the experimental one ( $\sigma_y^{exp} = 1.22 \pm 0.16$ ). The inverse slope of the predicted  $M_T$ - distribution, parameterized as  $dn_\phi/dM_T^2 dy \sim \exp(-M_T/T_\phi)$ ,  $T_\phi = 232 \pm 2$  MeV, is significantly smaller than the measured one  $T_\phi^{exp} = 305 \pm 15$  MeV. The recent attempt [14] to reproduce the  $M_T$ - distribution is also unsuccessful: the LUCIAE predictions prevail the data at small  $M_T - m_\phi < 0.15$  GeV/ $c^2$ , while at large  $M_T - m_\phi > 0.5$  GeV/ $c^2$  the predicted values are lower than the experimental ones.

This inconsistency at large  $M_T > 1.5$  GeV/ $c^2$  is more significant when comparing the model predictions with the NA50 data for the dimuon channel of  $\phi$  production in Pb+Pb collisions [7]. As seen from Fig. 3 (the left panel), the model predictions are 1.5-2 times lower of the data on the differential cross section integrated over the almost whole domain of impact parameter (except for the most peripheral collisions). The predicted value of  $T_\phi = 220 \pm 7$  MeV is, however, consistent with the measured one  $T_\phi^{exp} = 228 \pm 10$  MeV. Better agreement is obtained for the  $\rho + \omega$  differential cross section (Fig. 3, the right panel). Note, that the predicted values of the cross-sections (and of the multiplicities  $\langle n_\phi \rangle_{\mu\mu}$  and  $\langle n_{\rho+\omega} \rangle_{\mu\mu}$ , see below) are multiplied by a factor  $A_{CS} = 0.5$ , equal to the NA50 setup acceptance for the Collins-Soper angle. In this acceptance, the predicted inclusive cross section  $\sigma_{\rho+\omega}^{\mu\mu}$  (at  $1.5 < M_T < 3.5$  GeV/ $c^2$  and  $0 < y_{cm} < 1$ ) is equal to  $191 \pm 6 \mu b$  for the model option without the FSI, while, owing to the introduction of the latter, this value reaches  $240 \pm 8 \mu b$ , consistent with the measured one.

The dependence of the vector meson yield on the number  $N_{part}$  of participant nucleons in Pb+Pb collisions and that per participant nucleon,  $\langle n_\phi \rangle_{\mu\mu} / N_{part}$  and  $\langle n_{\rho+\omega} \rangle_{\mu\mu} / N_{part}$ , are plotted in Fig. 4. It is seen, that the model predicts an increasing yield per participant nucleon with increasing  $N_{part}$ , owing to the collective string mechanism incorporated into the model. However, this enhancement for  $\phi$  is much moderate than observed in the experiment [7]: the model predictions are lower of the data by a factor about 3 for the most central collisions (Fig. 4, the top panels). It should be stressed, that the model fails not only for the hidden strangeness sector, but also for the dimuon channel of the high- $M_T$   $\rho + \omega$  production. As seen from Fig. 4 (the bottom panels), the model predicts about 1.8 times smaller  $\langle n_{\rho+\omega} \rangle_{\mu\mu}$ , than measured in the most central collisions, while due to the introduction of the FSI this discrepancy reduces to about 1.4.

The model predictions concerning the  $\phi$ ,  $\rho$  and  $\omega$  production in 158 A GeV In+In collisions for the acceptance of the NA50/60 setup ( $0 < y_{cm} < 1$  and  $A_{CS} = 0.5$ ) are presented in Figs. 5 and 6. In this acceptance, the integrated over  $M_T$  cross sections are predicted to be  $\sigma_\phi^{\mu\mu} = 0.21 \text{ mb}$ ,  $\sigma_\rho^{\mu\mu} = 0.57 \text{ mb}$  and  $\sigma_\omega^{\mu\mu} = 0.83 \text{ mb}$  for the option without FSI, while  $\sigma_\phi^{\mu\mu} = 0.55 \text{ mb}$  and  $\sigma_\omega^{\mu\mu} = 1.09 \text{ mb}$  when the FSI is taken into account. It is seen from Fig. 5, that the  $N_{part}$ -dependence of  $\langle n_\phi \rangle$  and  $\langle n_\omega \rangle$  (when the FSI is taken into account for the latter) is significantly stronger, than that for  $\langle n_\rho \rangle$  (when the FSI is not taken into account) and for  $\langle n_\rho \rangle$ . The inverse slope parameter  $T$  (plotted in Fig. 6) for  $\phi$  is practically the same as for  $\rho$  and  $\omega$ , when the FSI is taken into account for the latters.

The predictions for p+A collisions ( $A \equiv \text{Be, Al, Cu, In, W, Pb, U}$ ) are presented, at  $0 < y_{cm} < 1$  and  $A_{CS} = 0.5$ , in Figs. 7 and 8. Again, owing to the collective string mechanism, the predicted mean multiplicity  $\langle n_\phi \rangle$  increases with  $A$  faster, than  $\langle n_\rho \rangle$  and  $\langle n_\omega \rangle$ . The ratio  $\langle n_\phi \rangle / \langle n_\omega \rangle$  for the heaviest target (U) exceeds by about 1.5 times that for pp collisions. The parameter  $A$  tends to increase with  $A$  (Fig. 8), being for  $\phi$  systematically higher as compared to that for  $\rho$  and  $\omega$ .

## 4 Summary

Predictions of the LUCIAE model, an updated version of the FRITIOF event generator, for the  $\rho, \omega, \phi$  production in proton-proton, proton-nucleus and nucleus-nucleus collisions at 158 A GeV are presented and compared with the available experimental data. The model parameters used for pp collisions were preliminary tuned by comparison with the data on the multiplicity distribution and inclusive spectra of charged particles and the strange particle yield in proton-proton (hadron-proton) interactions at the SPS energies.

The model predictions agree with the data [6] on the total average multiplicity  $\langle n_\phi \rangle$  and the ratio of  $\langle n_\phi \rangle / \langle n_\pi \rangle$  for pp, p+Pb and central Pb+Pb collisions, as well as approximately reproduces the  $M_T$  and  $y$  - distributions of  $\phi$  meson in pp collisions. However, for central Pb+Pb collisions, the model predicts more narrow  $y$  - spectrum and less steep  $M_T$  - distribution: the model overestimates by 30-50% the  $\phi$  yield at low  $M_T - m_\phi < 0.15$  GeV/ $c^2$  and underestimates by 20-40% that at higher  $0.6 < M_T - m_\phi < 1.1$  GeV/ $c^2$ . The predicted value of the inverse slope parameter  $T_\phi = 232 \pm 2$  MeV of the  $M_T$  - distribution turns out to be much smaller than the experimental one,  $T_\phi = 305 \pm 15$  MeV.

On the other hand, the model fits well the shape of the  $M_T$  - distribution for the dimuon channel of the  $\phi$  and  $\rho + \omega$  production in non-peripheral Pb+Pb collisions [7]. In the high  $M_T$  - region ( $1.5 < M_T < 3.2$  GeV/ $c^2$ ) the predicted values of  $T_\phi = 220 \pm 7$  MeV and  $T_{\rho+\omega} = 220 \pm 3$  MeV agree with experimental ones. The  $(\rho + \omega)$  yield is also reproduced by the model (when the FSI is included into the model), unlike that of  $\phi$  meson for which the predictions are 1.5-2 times lower than the data.

The situation worsens dramatically for central Pb+Pb collisions (for the high  $M_T$  region). The model badly underestimates not only the  $\phi$  yield (by a factor  $\sim 3$ ), but also that for  $(\rho + \omega)$  (by a factor  $\sim 2$ ). This discrepancy is less significant when comparing with the data [6] which concern the  $\phi \rightarrow K^+ K^-$  channel in the same range of  $M_T$ .

One can conclude, that the model fits, irrespective to  $N_{part}$ , the  $\phi$  total yield of  $\phi$  (for pp, p+Pb, Pb+Pb), but fails at high  $M_T$  region ( $M_T > 1.5$  GeV/ $c^2$ ), especially for the central Pb+Pb collisions for which, however, the magnitude of the discrepancy with data is rather different for different experiments [6, 7].

In conclusion, the LUCIAE model reproduces some features of the light vector meson production in proton-proton, proton-nucleus and nucleus-nucleus collisions at the SPS energies, but fails in describing the whole totality of the available data. Although the mechanism of the formation of multistring states in nuclear collisions, incorporated into the LUCIAE model, provides a strangeness enhancement, it turns out to be far from being sufficient to fit the data on the high- $M_T$   $\phi$  meson yield in the central heavy ion collisions. The final state interactions, introduced into the model, result in a significant increase of the  $\omega$  yield and lead to a better agreement with the experimental data.

## Acknowledgement

The authors are grateful to A.Grigoryan for useful discussions and comments. The work is partially supported by Calouste Gulbenkian Foundation and Swiss Fonds "Kidagan".

## References

- [1] J.Rafelsky and B.Muller, Phys. Rev. Lett. B48 (1982) 1066
- [2] A.Shor, Phys. Rev. Lett. 54 (1985) 1122
- [3] Sa Ben-Hao and Tai An, Comp. Phys. Comm. 90 (1995) 121;  
Tai An and Sa Ben-Hao, Comp. Phys. Comm. 116 (1999) 353
- [4] B.Andersson, G.Gustafson and Hong Pi, Z. Phys. C57 (1993) 485
- [5] Hong Pi, Comp. Phys. Comm. 71 (1992) 173
- [6] S.V.Afanasiev et al. (NA49 Coll.), Phys. Lett. B491 (2000) 59
- [7] M.C.Abreu et al. (NA50 Coll.), Phys. Lett. B555 (2003) 147
- [8] M.R.Atayan et al. (NA22 Coll.), Euro. Phys. J. C21 (2001) 271
- [9] B.Andersson and An Tai, Z. Phys. C71 (1996) 155
- [10] Tai An and Sa Ben-Hao, Phys. Lett. B409 (1997) 393
- [11] Ben-Hao Sa et al., Phys. Lett. B507 (2001) 104
- [12] Review of Particle Physics, Phys. Rev. D66 (2002) 010001-31
- [13] Review of Particle Physics, Euro. Phys. J. C15 (2000) 28
- [14] Ben Hao Sa et al., nucl-th/0205078, 2002

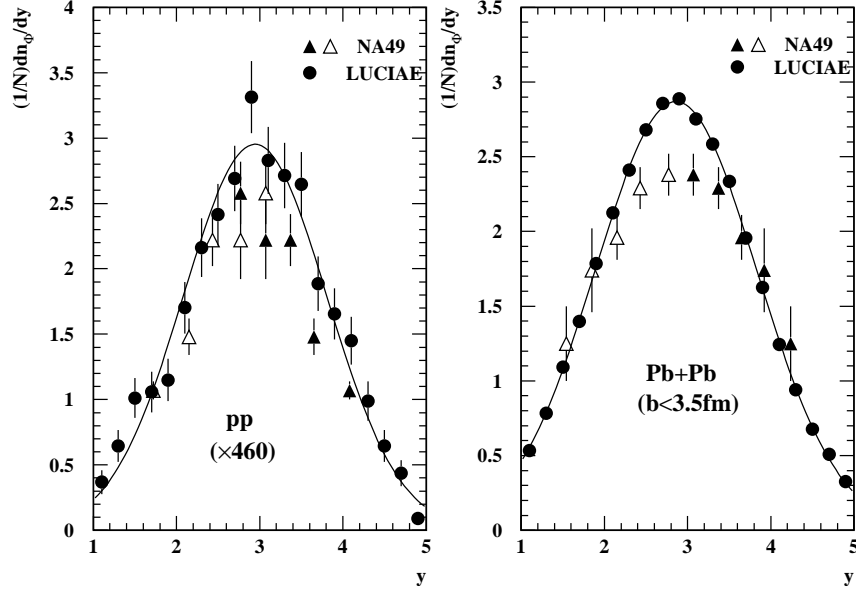


Figure 1: Rapidity distributions of  $\phi$  mesons in pp and Pb+Pb collisions. The curves are the result of the Gaussian fit of the simulated data.

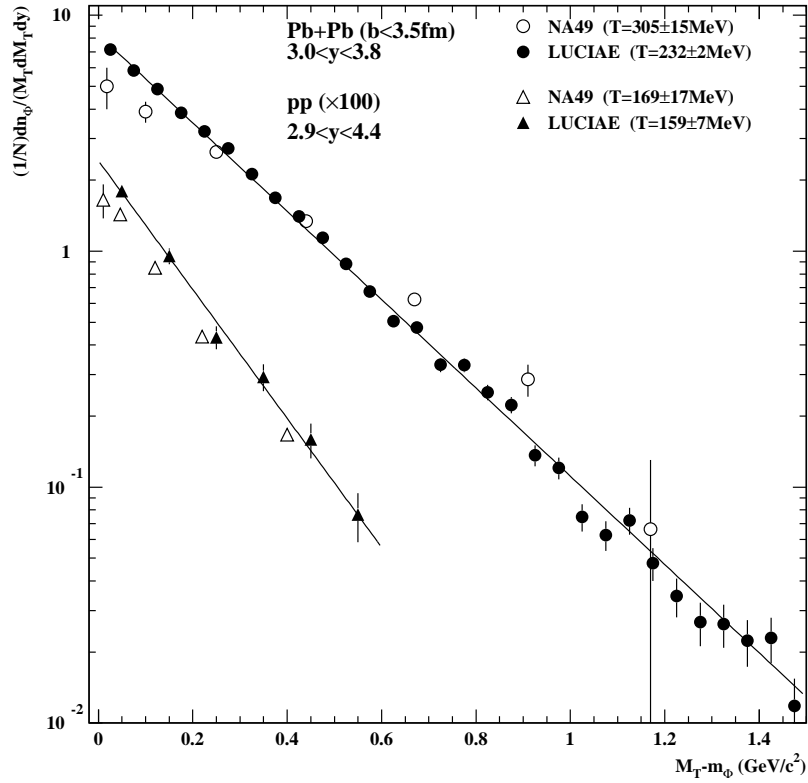


Figure 2: Transverse mass distribution of  $\phi$  mesons in pp and central Pb+Pb collisions. The curves are the result of the exponential fit of the simulated data.

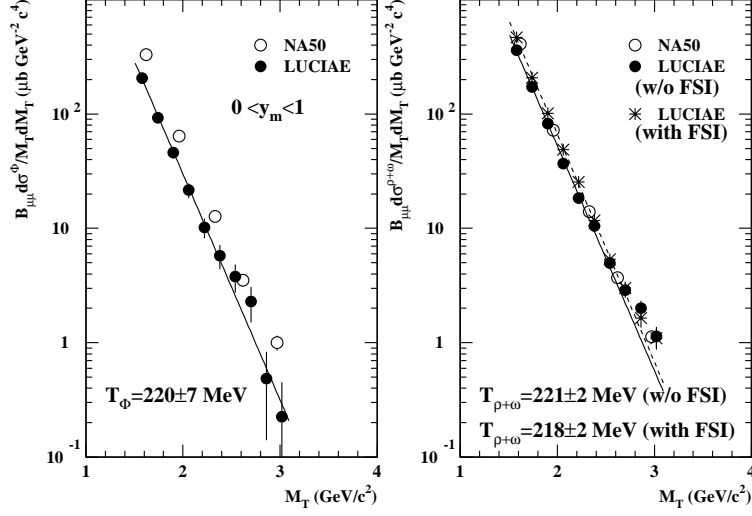


Figure 3: Transverse mass distributions of  $\phi$  and  $\rho + \omega$  in Pb+Pb collisions. The curves are the result of the fit(see text) of the simulated data without (solid lines) and with(dashed line) the FSI.

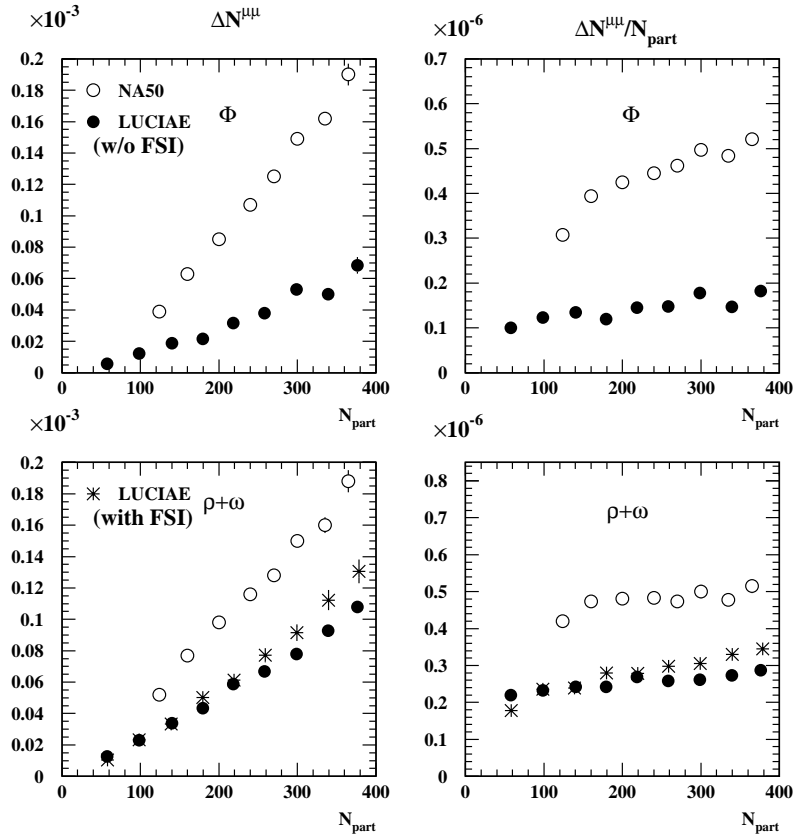


Figure 4: Multiplicities  $\langle n_\phi \rangle_{\mu\mu}$  and  $\langle n_{\rho+\omega} \rangle_{\mu\mu}$  (left panels) and multiplicities per participant nucleon (right panels) in Pb+Pb collisions.

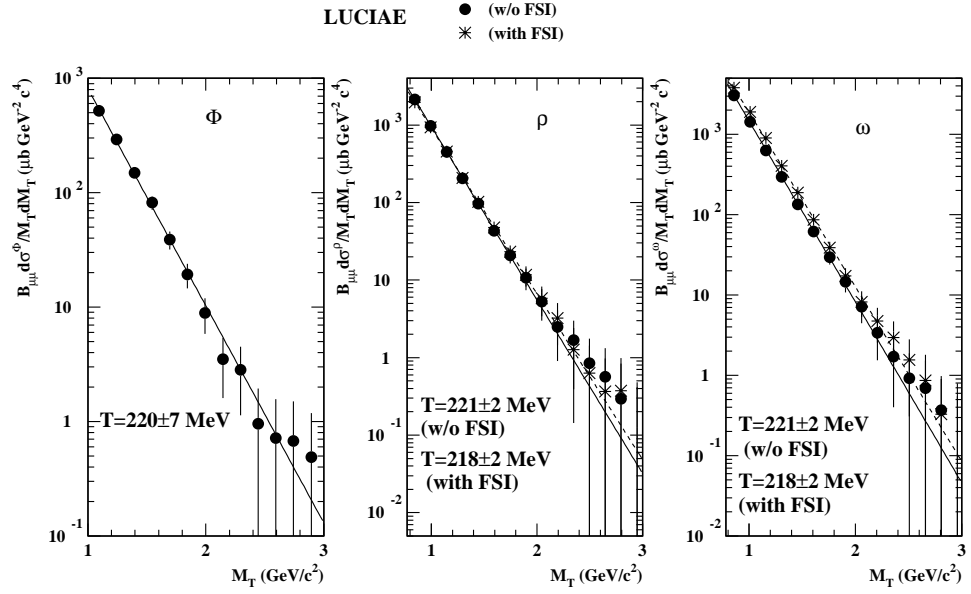


Figure 5: Transverse mass distributions of  $\phi$ ,  $\rho$  and  $\omega$  in In+In collisions. The curves are the result of the fit (see text) of the simulated data without (solid lines) and with (dashed line) the FSI.

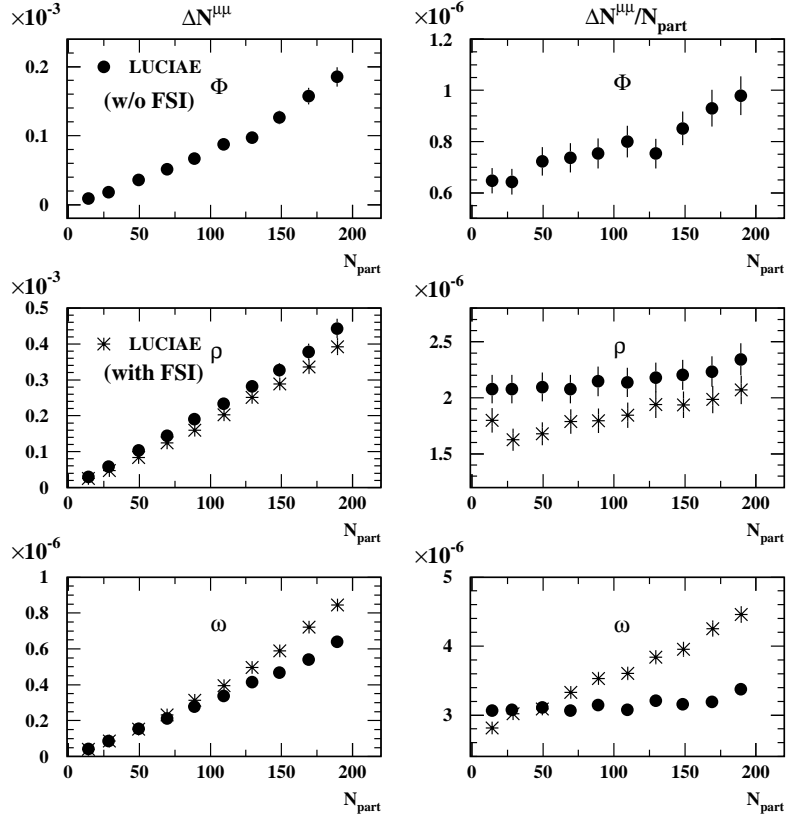


Figure 6: Mean multiplicities  $\langle n_\phi \rangle_{\mu\mu}$ ,  $\langle n_\rho \rangle_{\mu\mu}$  and  $\langle n_\omega \rangle_{\mu\mu}$  integrated over the whole  $M_T$  - region (left panels) and those per participant nucleon (right panels) in In+In collisions.

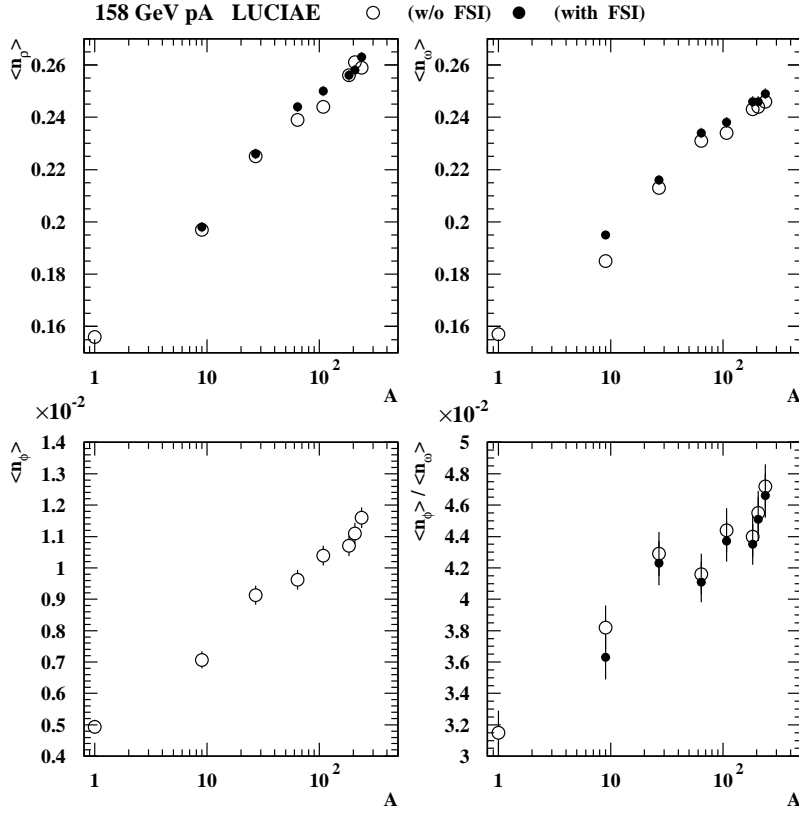


Figure 7: The A-dependence of the mean multiplicities  $\langle n_\rho \rangle$ ,  $\langle n_\omega \rangle$  and  $\langle n_\phi \rangle$  integrated over the whole  $M_T$  - region and the ratio  $\langle n_\omega \rangle / \langle n_\phi \rangle$  in p+A collisions.

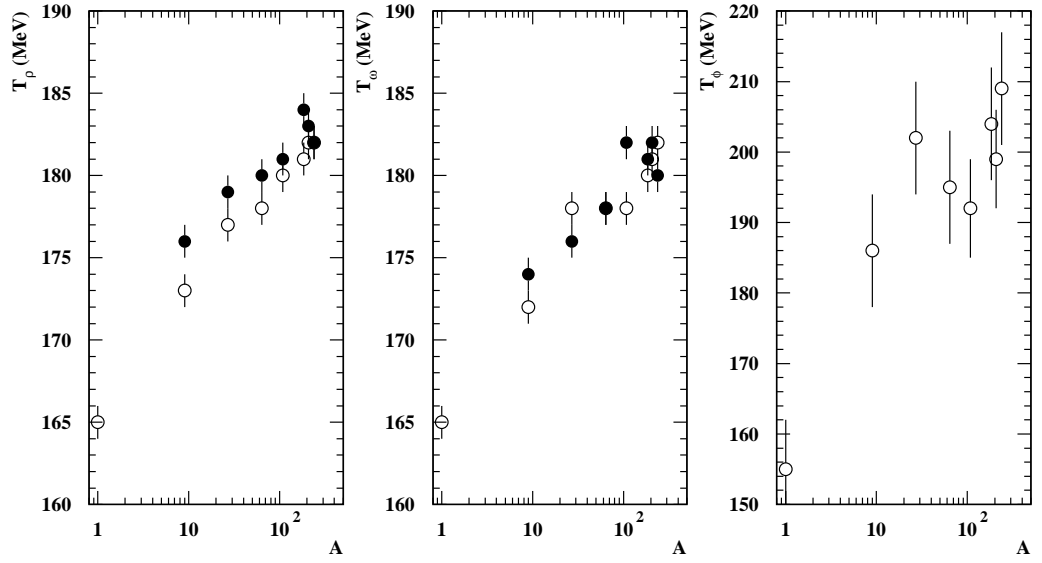


Figure 8: The A-dependence of the inverse slope parameters  $\langle T_\rho \rangle$ ,  $\langle T_\omega \rangle$  and  $\langle T_\phi \rangle$  of the  $M_T$  - distributions in p+A collisions.